HHS Public Access

Author manuscript

Gastroenterology. Author manuscript; available in PMC 2016 January 01.

Published in final edited form as:

Gastroenterology. 2015 January ; 148(1): 192–202.e3. doi:10.1053/j.gastro.2014.09.039.

Ablation of *Foxl1-Cre*-labeled hepatic progenitor cells and their descendants impairs recovery from liver injury

Soona Shin[1], **Naman Upadhyay**[1], **Linda E. Greenbaum**[2], and **Klaus H. Kaestner**[1]

[1]Department of Genetics and Institute for Diabetes, Obesity, and Metabolism, University of Pennsylvania School of Medicine, Philadelphia, PA 19104, USA

[2]Departments of Cancer Biology and Medicine, Thomas Jefferson University, Philadelphia, PA, 19107, USA

Abstract

BACKGROUND & AIMS—Foxl1$^+$ hepatic progenitor cells (HPCs) differentiate into cholangiocytes and hepatocytes following liver injury. We investigated the requirement for Foxl1+ HPCs in recovery from liver injury in mice.

METHODS—We developed mice in which we can trace and delete Foxl1-expressing HPCs and their descendants (Foxl1-Cre;RosaYFP/iDTR mice). Foxl1-Cre-negative mice were used as controls. Liver damage was induced in male mice by placing them on choline-deficient, ethionine-supplemented (CDE) diets for 15 days; mice were then placed on normal diets and allowed to recover. Liver damage was induced in female mice by placing them on 5-diethoxycarbonyl-1,4-dihydrocollidine-containing diets, followed by a recovery period. Some mice were given injections of diphtheria toxin mice during the recovery phase, to delete Foxl1-Cre–marked HPCs and their descendants. Livers were collected from all mice and analyzed by immunofluorescence, quantitative reverse transcription PCR, flow cytometry, and histologic analyses.

RESULTS—Foxl1-Cre-marked HPCs were required for development of cholangioctyes and hepatocytes in livers following CDE diet-induced injury. A smaller percentage of YFP$^+$ hepatocytes contained markers of oxidative stress, DNA damage, or cell death than YFP-negative hepatocytes, indicating that YFP$^+$ hepatocytes are newly formed cells. Injection of diphtheria

Correspondence: Klaus H. Kaestner, PhD, Department of Genetics and Institute for Diabetes, Obesity, and Metabolism, University of Pennsylvania School of Medicine,12-126 Translational Research Center, 3400 Civic Center Boulevard, Philadelphia, PA 19104. kaestner@mail.med.upenn.edu; fax: +1-215-573-5892..

*Current address: Janssen R&D, LLC; Spring House, PA

Disclosures: The authors disclose no conflicts.

Author Contributions: SS: study concept and design; acquisition of data; analysis and interpretation of data; drafting of the manuscript; statistical analysis; obtained funding.

NU: acquisition of data; analysis and interpretation of data; editing of the manuscript. LEG: study concept and design; editing of the manuscript.

LEG: study concept and design; editing of the manuscript.

KHK: study concept and design; analysis and interpretation of data; drafting of the manuscript; obtained funding; study supervision.

toxin deleted YFP$^+$ cells from Foxl1-Cre;RosaYFP/iDTR mice and prevented the resolution of hepatic steatosis. In mice recovering from dihydrocollidine-containing diet-induced injury, most cholangiocytes arose from Foxl1-Cre-marked HPCs. Deletion of YFP+ cells did not alter levels of markers of liver injury or liver function.

CONCLUSIONS—Based on studies of Foxl1-Cre;RosaYFP/iDTR mice, Foxl1+ HPCs and/or their descendants are required for development of cholangioctyes and hepatocytes in liver following CDE diet-induced injury.

Keywords

HPCs; oval cells; choline-deficient, ethionine-supplemented diet

Hepatic progenitor cells (HPCs), also known as oval cells in rodents, are the epithelial component of the ductular reaction that proliferates in response to chronic liver injury.[1] Although previous studies demonstrated that the HPC compartment expands during injury and that HPCs differentiate into cholangiocytes and hepatocytes in culture,[2,3] only a very small number of hepatocytes were formed from HPCs *in vivo* following liver injury caused by either 3,5-diethoxycarbonyl-1,4-dihydrocollidine-containing diet (DDC) or bile-duct ligation.[4] Therefore, definitive evidence demonstrating that HPCs are required for liver regeneration and restoration of metabolic function is still lacking.

In 2012, Español-Suñer and colleagues employed genetic lineage tracing to determine under which conditions osteopontin-expressing cholangiocytes and HPCs contribute to restoration of hepatocyte mass.[5] Osteopontin-marked cells did not contribute significantly to hepatocytes during normal homeostatic conditions, or after partial hepatectomy, DDC or carbon tetrachloride treatment.[5] However, in mice fed a choline-deficient, ethionine-supplemented (CDE) diet, 2.45% of hepatocytes were derived from osteopontin-marked cells after the mice were allowed to recover on normal chow. The CDE diet impairs hepatocyte function by preventing triglyceride export, thereby causing steatosis,[6] peroxidation of phosphatidylcholine,[7] inflammation,[8] and transient mitotic arrest of hepatocytes.[9] Thus, the study by Español-Suñer and colleagues suggested that osteopontin-expressing progenitor cells contribute to homeostatic repair following liver injury.

To date it is not known to which degree progenitor cells are required for or important in this recovery from CDE-mediated liver injury. We previously demonstrated that *Foxl1-Cre* is a marker of HPCs found in the injured liver, and that *Foxl1-Cre* marked cells can be isolated, expanded, and differentiated towards both the cholangiocyte and hepatocyte lineages in vitro.[3,4] To address the issue of whether HPCs contribute to the recover from liver injury in vivo, we developed a new mouse model in which we could both trace and ablate *Foxl1*-expressing HPCs and their descendants. In this model, the *Foxl1-Cre* transgene effects recombination of two alleles in the *Rosa26* locus, one leading to production of yellow fluorescent protein (YFP), the other to the expression of the diphtheria toxin receptor (DTR) on the cell surface of the targeted cells.[10-12] Thus, *Foxl1-Cre* marked HPCs and their descendants can be ablated at will through administration of diphtheria toxin (DT), to which mouse cells are normally resistant.[11,12] Using this new model, we show that *Foxl1-Cre*

marked HPCs are indeed important in the restoration of liver function following injury, but also that this requirement depends on the specific type of injury imparted on the liver.

Materials and Methods

Mice

For lineage-tracing studies, *Foxl1-Cre* mice[13] were crossed to *Rosa*^{YFP} reporter mice[10] and Creinducible diphtheria toxin receptor (DTR) (*Rosa*^{iDTR}) mice.[12] To induce liver injury, male mice (4-6 weeks of age) were treated with a choline-deficient diet (MP Biomedicals, Santa Ana, CA) and drinking water containing 0.15% ethionine[5] and 5% sucrose for 15 days. *Foxl1-Cre*-negative mice were used as controls. For ablation of *Foxl1-Cre*-labeled cells, mice were injected with 500 ng of diphtheria toxin (DT, Sigma-Aldrich, St. Louis, MO) twice per day for 4 days after completion of the CDE diet.[11,14] Female mice (4-5 weeks of age) were fed a diet containing 0.1% DDC (Harlan Laboratories, Indianapolis, IN) for 14 days.[4] 500 ng of DT combined with a DDC diet resulted in toxicity in *Foxl1-Cre*-negative control mice. Therefore, for ablation of *Foxl1-Cre*-labeled cells in this model, mice were injected with 250 ng DT twice daily for 3 days after completion of the DDC diet. Mice were sacrificed 16 hours after the last injection. All protocols were approved by the Institutional Animal Care and Use Committee of the University of Pennsylvania.

Immunofluorescence Staining

See the Supplementary Materials and Methods section.

Cell Counting

For quantification of cell numbers, twelve random pictures centered on the portal triad were taken. Approximately 1,000 cholangiocytes and 750 hepatocytes were counted per mouse. All CK19-expressing populations, which include mature pre-existing cholangiocytes and HPCs, are referred to as “cholangiocytes” in the figures. Hepatocytes were detected based on HNF4α staining and/or morphology.

Oil-Red-O Staining

See the Supplementary Materials and Methods section.

Hepatic Triglyceride Measurements and Biochemical Analyses of Plasma

See the Supplementary Materials and Methods section.

RNA Isolation and Quantitative RT-PCR Analyses

See the Supplementary Materials and Methods section.

Isolation of YFP^{+} Hepatocytes Using a Fluorescence-Activated Flow Cytometry Cell Sorter (FACS) and Culture of Hepatocytes

Isolation of primary hepatocytes from livers was performed according to the two-step collagenase perfusion protocol.[15] See the Supplementary Materials and Methods section for details.

Statistical Analyses

Student t-tests were used to determine the significance of differences between two groups. A *P* value of 0.05 was considered statistically significant.

Results

Foxl1-Cre-Marked Cells Contribute to the Liver Parenchyma after CDE diet-Induced Injury

Given the observation from Español-Suñer and colleagues that osteopontin-marked progenitors are most efficiently recruited to replace hepatocytes in the CDE diet model,[5] we first tested to which degree *Foxl1*-expressing cells contribute to the liver parenchyma in this paradigm. We treated *Foxl1-Cre*;*Rosa*$^{YFP/iDTR}$ mice with the CDE diet for 15 days and then let the mice recover for 4 days on normal chow (Figure 1A). We observed that expression of YFP was detected only in the livers of mice that lost more than 14% of their initial body weight one week after exposure to CDE diet, while mice that had retained weight showed no activation of *Foxl1*-marked HPCs (data not shown). Furthermore, the mice that lost more than 14% of their initial body weight also had plasma levels of the liver injury maker alanine aminotransferase (ALT) (218 ± 43 U/L, n = 5) that were higher than those of mice that lost less than 14% of their initial body weight (153 ± 30 U/L, n = 3, *P* = .06). These findings are consistent with the observation that the extent of the ductular reaction correlates with the severity of liver injury in humans.[16] Therefore, we only included mice that lost more than 14% of their initial body weight after exposure to CDE diet in this study.

We harvested liver directly after the injury period (d15) or after a 4 day recovery period (d19). While 18% of CK19$^+$ cholangiocytes and 5% of HNF4α$^+$ hepatocytes were marked by YFP in the liver of *Foxl1-Cre*;*Rosa*$^{YFP/iDTR}$ mice at d15 (Figure 1B and C), more than 50% of CK19$^+$ cholangiocytes and 29% of HNF4α$^+$ hepatocytes were marked by YFP in the liver of *Foxl1-Cre*;*Rosa*$^{YFP/iDTR}$ mice after the recovery period at d19 (Figure 1B and C). We did not detect any YFP-expressing cells in the livers of normal chow-fed *Foxl1-Cre*;*Rosa*$^{YFP/iDTR}$ mice and CDE-fed *Rosa*$^{YFP/iDTR}$ control mice (Figure 1B). These results indicate that CDE-mediated liver injury led to induction of *Foxl1-Cre* expression, and that *Foxl1-Cre*-labeled cells produced both cholangiocytes and hepatocytes, in agreement with the report by Español-Suñer et al.[5]

To investigate whether the increase in the number of YFP$^+$ cells after the recovery period is attributable to increased proliferation, liver sections were stained with an anti-Ki67 antibody. The CDE diet caused a massive proliferative response in both cholangiocytes and hepatocytes at day 19, as detected by Ki67 staining of replicating cells (Figure 1D and E). While proliferation rates of cholangiocytes remained similar between days 15 and 19, proliferation rates of hepatocytes were dramatically increased after the recovery period (Figure 1E). Next, we quantified the percentage of Ki67$^+$ cells in YFP$^+$ and YFP$^-$ populations separately. While proliferation rates were similar between *Foxl1-Cre*/YFP$^+$ and YFP$^-$ cells at day 15, proliferation rates of YFP$^+$ cells were significantly higher than proliferation rates of YFP$^-$ cells at day 19 (Figure 1F). Thus, our results indicate that *Foxl1-Cre*$^+$ HPCs and their descendants contribute to the proliferative response following CDE-mediated liver injury.

Foxl1-Cre-Marked YFP$^+$ Hepatocytes Are Newly Formed Cells

One caveat with the current model is the fact that we employed *Foxl1-Cre* mice, and not a tamoxifen-inducible CreER transgene driven by the same promoter/enhancer, as this is not available. Thus, it is formally possible that pre-existing hepatocytes activated the *Foxl1-Cre* promoter sometime during the course of the CDE paradigm, and became YFP$^+$ by this route. Based on the fact that the CDE diet leads to increased oxidative stress[17] and lipid peroxidation,[7] we hypothesized that if YFP$^+$ hepatocytes are newly formed cells, they will be exposed to oxidative stress for a shorter time period than pre-existing YFP$^-$ hepatocytes (Figure 2A). Therefore, we stained liver sections for the presence of 4-hydroxy-2-nonenal (4-HNE), a toxic product derived from lipoperoxidation.[18] As shown in Figure 2B, YFP$^+$ and YFP$^-$ hepatocytes were not equivalent, as the percentage of cells labeled with 4-HNE was higher in YFP$^-$ hepatocytes compared to YFP$^+$ hepatocytes. We also performed staining for γH2AX, a marker of DNA damage caused by double strand breaks, and terminal deoxynucleotidyl transferase dUTP nick end labeling (TUNEL), as oxidative stress causes DNA fragmentation and cell death.[19] While a fraction of YFP$^-$ hepatocytes was labeled with γH2AX or TUNEL (Figure 2C and D), we did not detect any YFP$^+$ hepatocytes labeled with these markers. We observed no 4-HNE, γH2AX, and TUNEL-marked cells in CK19$^+$ populations, indicating that CDE-induced injury is primarily affecting hepatocytes.

To rule out the possibility that YFP$^-$ hepatocytes are more susceptible to oxidative stress than YFP$^+$ hepatocytes, we isolated YFP$^-$ and YFP$^+$ hepatocytes from viable fraction of hepatocytes using flow cytometry and placed them in culture. Cells were treated with hydrogen peroxide (H_2O_2), which has been shown to cause accumulation of 4-HNE and γH2AX, eventually leading to cell death.[19,20] As demonstrated in Figure 2E, H_2O_2-caused cytotoxicity was not different between the two groups, indicating that YFP$^-$ and YFP$^+$ hepatocytes are equally susceptible to oxidative stress. Therefore, our findings suggest that the percentage of stress marker-labeled YFP$^+$ hepatocytes is small compared to YFP$^-$ hepatocytes because they are newly formed cells, and have thus been exposed to a toxic environment for only a short time period.

Our previous report demonstrated that *Foxl1* mRNA levels were decreased when HPCs were differentiated into hepatocytes in culture.[3] Therefore, we investigated whether expression of Cre recombinase is decreased in YFP$^+$ hepatocytes *in vivo* (Supplementary Figure 1A). Expression of Cre was restricted to CK19$^+$YFP$^+$ cholangiocytes (Supplementary Figure 1B), while YFP$^+$ hepatocytes did not express Cre. Although we cannot completely rule out the possibility that YFP$^+$ hepatocytes may have expressed Cre recombinase transiently, or that levels of Cre are below the detection limit in YFP$^+$ hepatocytes, these data combined with the results shown in Figure 2 strongly support the notion that YFP$^+$ hepatocytes are newly formed cells derived from CK19$^+$YFP$^+$Cre$^+$ cells.

We detected Cre expression in CK19$^+$ cells with normal ductal morphology as well as in atypical ductal cells with small or no lumen, implying that mature cholangiocytes that express Cre in response to injury become progenitor cells. We hypothesized that if HPCs are converted into hepatocytes, we will observe an increase in the number of YFP$^+$ hepatocytes with a decrease in the number of HPCs between days 15 and 19. However, as expression of

Cre in $CK19^+$ population was maintained after the recovery phase (Supplementary Figure 1B and C), we did not see a decrease in the number of $CK19^+YFP^+Cre^+$ cells between day 15 and day 19, although the number of YFP^+ hepatocytes was increased (Supplementary Figure 1C and Figure 1C). One possible explanation for this finding is that YFP^+ cholangiocytes undergo asymmetric cell division, with only one of the daughter cells contributing to hepatocytes, while the other remains in the biliary epithelium.

Foxl1-Cre-Marked Cells Are Required for Recovery from Liver Injury Caused by CDE diet

Having established that *Foxl1*-marked cells constitute a large fraction of the liver mass following CDE diet, we could now assess if *Foxl1*-expressing HPCs and their descendants are required for the liver's ability to recover from injury. Injection of *Foxl1-Cre*;$Rosa^{YFP/iDTR}$ mice with DT only during the recovery phase (Figure 3A) led to 83% ablation of marked cholangiocytes and 99% ablation of marked hepatocytes (Figure 3B and C). We observed that DT-injected *Foxl1-Cre*;$Rosa^{YFP/iDTR}$ mice had paler livers compared to saline-injected mice after the 4 day recovery period (Figure 3D). Oil-Red-O staining for neutral lipids and quantification of hepatic triglyceride content showed persistent steatosis only in DT-treated *Foxl1-Cre*;$Rosa^{YFP/iDTR}$ mice, but not in saline-treated *Foxl1-Cre*;$Rosa^{YFP/iDTR}$ mice or in DT-treated $Rosa^{YFP/iDTR}$ control mice (Figure 3E and F).

In addition, we assessed biochemical markers of liver injury and function (Figure 4A). We measured plasma levels of markers of hepatocellular injury, i.e. aspartate aminotransferase (AST) and alanine aminotransferase (ALT), and markers of cholestatic injury, i.e. alkaline phosphatase (ALP) and gamma-glutamyltransferase (GGT). Albumin is a marker of liver function, and elevated total bilirubin levels indicate liver injury and/or impaired liver function.[21] We observed trends toward prolonged injury and impaired liver function after DT-mediated cell ablation, although changes were not statistically significant due to the high variability between individual mice. Surprisingly, the total number of $Ki67^+$ hepatocytes remained unaltered after DT administration (Figure 4B), suggesting that YFP^- hepatocytes proliferate to compensate for the loss of YFP^+ hepatocytes. In sum, our results provide strong evidence that the role of HPCs is to provide undamaged newly formed hepatocytes during the recovery phase that can meet increased metabolic demands after liver injury.

We next asked whether YFP^+ cells were required for the proliferative response and function of cholangiocytes. Our Ki67 staining indicates that the total number of $Ki67^+$ cholangiocytes was decreased after DT administration (Figure 4B). The mRNA levels of several functional markers of cholangiocytes[22,23] anion exchanger 2 (*Slc4a2*), cystic fibrosis transmembrane conductance regulator (*Cftr*), and aquaporin 5 (*Aqp5*) were decreased after DT administration (Supplementary Figure 2B), consistent with the reduction in cholangiocyte number. These results indicate that YFP^+ cholangiocytes are required for the proliferative response and restoration of cholangiocyte number after injury. However, the fact that that there were no significant changes in the levels of ALP and GGT (Figure 1A) indicates that there is no major impairment of bile flow. In sum, our results indicate that *Foxl1-Cre*/YFP^+ cells are required for providing healthy hepatocytes and cholangiocyte proliferation during the recovery phase.

Foxl1-Cre-Marked Cells Contribute to Cholangiocytes after DDC Diet-Induced Liver Injury

To determine whether *Foxl1-Cre*-marked cells are required in another injury model, we treated *Foxl1-Cre*;*Rosa*$^{YFP/iDTR}$ mice with a DDC diet[1,3,4] for 14 days and then let the mice recover for 3 days on normal chow (Figure 5A). We harvested liver after the injury period (d14) and after the 3 days of recovery period (d17). 8% and 11% of CK19$^+$ cholangiocytes were marked by YFP at day 14 and day 17 respectively in the liver of *Foxl1-Cre*;*Rosa*$^{YFP/iDTR}$ mice (Figure 5B and C). We did not detect any YFP$^+$HNF4α$^+$ hepatocytes at d14, and only 0.1% of HNF4α$^+$ hepatocytes were marked by YFP at d19. These results are consistent with previous studies that have demonstrated that *Foxl1-Cre*-marked cells and osteopontin-marked cells minimally contribute to hepatocytes after DDC treatment.[4,5] We next stained liver sections with Ki67 to detect replicating cells. While proliferation rates of cholangiocytes remained unchanged between day 14 and day 17, proliferation of hepatocytes was dramatically increased after the recovery period (Figure 5D and E). These results suggest that both CDE diet and DDC diet inhibit hepatocyte proliferation during the injury period, and hepatocytes are released from mitotic arrest during the recovery period. Proliferation rates of YFP$^+$ cholangiocytes were slightly higher than those of YFP$^-$ cholangiocytes at day 14 and day 17 (Figure 5F).

Next, we assessed if *Foxl1*-expressing HPCs and their descendants are required for recovery from DDC-induced liver injury. Injection of *Foxl1-Cre*;*Rosa*$^{YFP/iDTR}$ mice with DT only during the recovery phase (Figure 6A) led to 71% ablation of marked cholangiocytes (Figure 6B and C). There was no differenced between groups at day 17 in terms of hepatocellular injury as assessed by plasma AST and ALT levels, consistent with our findings that YFP$^+$ cells contribute primarily to cholangiocytes but not to hepatocytes in this injury model (Figure 7A). There was a trends toward cholestatic injury after ablation as indicated by plasma levels of GGT, although changes were not statistically significant (Figure 7A). Interestingly, albumin levels were increased at day 14 and decreased after recovery. This is perhaps due to the fact that the DDC diet causes liver enlargement.[24] The total number of Ki67$^+$ cholangiocytes and hepatocytes remained unaltered after DT administration (Figure 7B), suggesting that YFP-marked cells are not required for the proliferative response in this model. In sum, our results demonstrate that *Foxl1-Cre*-labeled HPCs and their descendants do not make a substantial contribution to recovery from DDC-induced liver injury.

Discussion

This study provides evidence that HPCs and their descendants are required for the recovery from specific types of liver injury, using our novel approach of combining *Foxl1-Cre*-driven cell lineage labeling and cell ablation. While multiple reports have demonstrated the existence of HPCs *in vivo* and bipotential differentiation capabilities of HPCs into cholangiocytes and hepatocytes differentiation *in vitro*,[1,25] our study is the first to demonstrate extensive contribution of HPCs to the liver parenchyma following liver injury and a specific requirement for HPCs during the recovery phase.

Our results are in a good agreement with the findings published by Español-Suñer and colleagues,[5] as the percentage of HPC-derived hepatocytes dramatically increased during the recovery phase in the liver of CDE-treated mice, while the percentage of progenitor-derived

hepatocytes was negligible in the livers of DDC-fed mice. However, the number of *Foxl1-Cre*-marked hepatocytes was much higher than that of OPN-iCreER^{T2}-labeled hepatocytes (29% versus 2.45%, respectively).[5] There are two likely explanations for this discrepancy. First, OPN-iCreER^{T2} did not label all the cells expressing osteopontin,[5] therefore the actual number of progenitor-derived hepatocytes is expected to be higher than 2.45%. Second, it is possible that *Foxl1-Cre* labels a wider population than OPN-iCreER^{T2}.

A recent study using a different approach for lineage tracing reported that the number of hepatocytes derived from non-hepatocyte origins was minimal in the CDE model.[26] Importantly, while we used 0.15% ethionine water to induce liver injury, 0.1% ethionine water was employed in that study. This is in line with our finding that it is critical to control for the severity of liver injury, as those mice that did not lose a significant fraction of their body weight on the CDE diet did not activate the progenitor cell response. Our study is also in agreement with the recent studies performed using zebrafish models by two independent groups, where extensive conversion of cholangiocytes into hepatocytes were observed only after massive depletion of hepatocytes.[27,28] We also found that it is critical to singly-house the mice on the CDE diet, in order to control for the amount of food and DL-ethionine water consumed by each mouse. We also added sucrose to the DL-ethionine water to improve its palatability. Sucrose is known to exacerbate steatohepatisis when combined with a methionine-choline-deficient diet by promoting de novo lipogenesis and triglycerides synthesis.[29] In sum, our findings indicate that it is critical to induce severe liver injury beyond a certain threshold to activate the Foxl1-Cre progenitor response in mice. In rat, inhibition of hepatocyte proliferation by 2-acetylaminofluorene after partial hepatectomy is a prerequisite for the activation of progenitor cell compartment.[30] In contrast, mouse hepatocytes are resistant to mitoinhibition as compared to rat and human hepatocytes,[31] and both CDE and DDC diets did not completely block hepatocyte proliferation in this study, underscoring the importance of controlling the severity of liver injury in mouse models.

In contrast, the number of YFP-marked hepatocytes remained very low in DDC-fed mice even after the recovery phase. To date, CDE diet seems to be the only way to induce the extensive conversion of HPCs to hepatocytes, given the lack of substantial contributions of HPC-derived hepatocytes to parenchyma using other models such as partial hepatectomy, DDC, carbon tetrachloride, and bile duct ligation.[4,5] While our findings demonstrate that the degree of injury is an important determinant for the activation of the progenitor compartment in CDE-fed mice, mice fed a DDC diet for 2 weeks had comparable levels of AST and ALT to CDE-fed mice, and levels of ALP and bilirubin were even high as compared to CDE-fed mice. One possible explanation is differential accumulation of extracellular matrix in response to CDE and DDC diets, as thick laminin layers inhibit escape of progenitor cells into parenchyma in DDC-fed mice.[5] In addition, since DDC diet causes hepatic porphyria[32] while CDE diet leads to steatosis,[6,33] signaling cascades triggered by the DDC diet are expected to be different from the ones activated in the CDE model. Further studies will be required to elucidate the molecular mechanisms underlying the difference between CDE models and other models of liver diseases.

Our results suggest that one role of HPCs is to supply newly formed hepatocytes that can remove excessive fat accumulated during the injury phase. Immunofluorescence staining for

stress makers provides strong evidences that the CDE diet causes primarily hepatocytic injury. Therefore, cholangiocytes that remained undamaged during the injury phase were able to supply HPC-derived healthy hepatocytes. Although YFP^+ cells had high proliferation rates compared to YFP^- cells, ablation of YFP^+ cells did not alter the total number of $Ki67^+$ hepatocytes. Therefore, our study suggests that the primary role of HPCs is to supply healthy hepatocytes following injury rather than to restore hepatocyte mass. Our biochemical analyses also support this notion, as we did not see dramatic changes in the plasma levels of indicators of liver injury and function markers after ablation of Foxl1-Cre marked cells. However, albumin levels, which were used to gauge liver function, may not be informative because its half-life is 2-3 weeks.[21] Our results also indicate that the livers of CDE-fed mice are not fully recovered after 4 days on normal chow, as evidenced by high AST and ALT levels at day 19 compared to control mice. Therefore, a prolonged injury phase combined with DT administration may reveal larger alteration in biochemical markers after ablation. Nonetheless, we saw a dramatic increase in lipid accumulation after ablation, supporting our hypothesis that HPCs are required for recovery.

In addition, while our study primarily focused on HPC-derived hepatocytes, ablation of YFP-marked cells decreased the number of total proliferating cholangiocytes, indicating that HPCs are also required for the proliferative response of biliary epithelia. It still remains unclear whether HPC-derived cholangiocytes are required for restoration of liver function. We did not observe significant changes in injury/function markers after ablation in mice treated with DDC diet where YFP-labeled hepatocytes were rarely found. However, since we were not able to completely ablate YFP^+ cholangiocytes even at maximum dose of DT without toxicity, it is possible that the remaining YFP^+ cholangiocytes were sufficient to perform their required functions.

In sum, our results demonstrate that the recovery of the liver from CDE diet-induced steatosis is markedly impaired following ablation of *Foxl1*-expressing HPCs and their descendants. One limitation of our study, as we mentioned earlier, is that we used *Foxl1-Cre* instead of an inducible CreER system. To address this issue, we provided multiple pieces of evidence demonstrating that YFP^+ hepatocytes are newly formed cells. We also observed that Cre expression is strictly restricted to the biliary compartment. Although these findings suggest that mature cholangiocytes that express *Foxl1* become progenitor cells, and that YFP^+ hepatocytes originate from HPCs, we cannot completely rule out the possibility that *Foxl1-Cre* is transiently expressed in mature hepatocytes. Nevertheless, even in this alternative scenario only a minority of hepatocytes activates *Foxl1*, and this subset of hepatocytes is essential for the recovery from liver injury. This study is the first to suggest that *Foxl1*-expressing HPCs are required to produce healthy hepatocytes that are different from pre-existing hepatocytes, and that ablation of HPCs and their descendants impairs the recovery of the liver from toxic injury.

Supplementary Material

Refer to Web version on PubMed Central for supplementary material.

Acknowledgements

We thank Tia Bernard-Banks (University of Pennsylvania) for managing the mouse colony, Dr. Kirk Wangensteen (University of Pennsylvania) and Dr. Monica Teta-Bissett (University of Pennsylvania) for their technical assistance, Dr. Fabrizio Thorel (University of Geneva) for providing the protocol for injecting diphtheria toxin, Michael Ray (Vanderbilt University) and Dr. Christopher V. Wright (Vanderbilt University) for providing the protocol for immunofluorescence staining, and Dr. Joshua R Friedman (University of Pennsylvania) for providing the anti-CK19 antibody. These studies were facilitated by Molecular Pathology and Imaging Core of the Penn Center for Molecular Studies in Digestive and Liver Disease (P30-DK50306) and the Flow Cytometry and Cell Sorting Resource Laboratory.

Grant Support: This work was supported by the American Association for the Study of Liver Diseases/American Liver Foundation Liver Scholar Award to SS and the National Institutes of Health P01-DK049210 to KHK.

Abbreviations used in this paper

CDE diet	choline-deficient, ethionine-supplemented diet
DAPI	4′,6-diamidino-2-phenylindole
4-HNE	4-hydroxy-2-nonenal
HPCs	hepatic progenitor cells
iDTR	Cre-inducible ditphtheria toxin receptor
YFP	yellow fluorescent protein
LDH	lactate dehydrogenase
AST	aspartate aminotransferase
ALT	alanine aminotransferase
ALP	alkaline phosphatase
GGT	gamma-glutamyltransferase

References

1. Shin S, Kaestner KH. The origin, biology, and therapeutic potential of facultative adult hepatic progenitor cells. Curr Top Dev Biol. 2014; 107:269–292. [PubMed: 24439810]
2. Okabe M, Tsukahara Y, Tanaka M, et al. Potential hepatic stem cells reside in EpCAM+ cells of normal and injured mouse liver. Development. 2009; 136:1951–1960. [PubMed: 19429791]
3. Shin S, Walton G, Aoki R, et al. Foxl1-Cre-marked adult hepatic progenitors have clonogenic and bilineage differentiation potential. Genes Dev. 2011; 25:1185–1192. [PubMed: 21632825]
4. Sackett SD, Li Z, Hurtt R, et al. Foxl1 is a marker of bipotential hepatic progenitor cells in mice. Hepatology. 2009; 49:920–929. [PubMed: 19105206]
5. Español-Suñer R, Carpentier R, Van Hul N, et al. Liver progenitor cells yield functional hepatocytes in response to chronic liver injury in mice. Gastroenterology. 2012; 143:1564–1575. [PubMed: 22922013]
6. Lombardi B, Pani P, Schlunk FF. Choline-deficiency fatty liver: impaired release of hepatic triglycerides. J Lipid Res. 1968; 9:437–446. [PubMed: 5725875]
7. Yoshida LS, Miyazawa T, Hatayama I, et al. Phosphatidylcholine peroxidation and liver cancer in mice fed a choline-deficient diet with ethionine. Free Radic Biol Med. 1993; 14:191–199. [PubMed: 8425721]
8. Knight B, Yeoh GC. TNF/LTalpha double knockout mice display abnormal inflammatory and regenerative responses to acute and chronic liver injury. Cell Tissue Res. 2005; 319:61–70. [PubMed: 15592751]

9. Dumble ML, Croager EJ, Yeoh GC, et al. Generation and characterization of p53 null transformed hepatic progenitor cells: oval cells give rise to hepatocellular carcinoma. Carcinogenesis. 2002; 23:435–445. [PubMed: 11895858]
10. Srinivas S, Watanabe T, Lin CS, et al. Cre reporter strains produced by targeted insertion of EYFP and ECFP into the ROSA26 locus. BMC Dev Biol. 2001; 1:4. [PubMed: 11299042]
11. Thorel F, Nepote V, Avril I, et al. Conversion of adult pancreatic alpha-cells to beta-cells after extreme beta-cell loss. Nature. 2010; 464:1149–1154. [PubMed: 20364121]
12. Buch T, Heppner FL, Tertilt C, et al. A Cre-inducible diphtheria toxin receptor mediates cell lineage ablation after toxin administration. Nat Methods. 2005; 2:419–426. [PubMed: 15908920]
13. Sackett SD, Fulmer JT, Friedman JR, et al. Foxl1-Cre BAC transgenic mice: a new tool for gene ablation in the gastrointestinal mesenchyme. Genesis. 2007; 45:518–522. [PubMed: 17661401]
14. Saito M, Iwawaki T, Taya C, et al. Diphtheria toxin receptor-mediated conditional and targeted cell ablation in transgenic mice. Nat Biotechnol. 2001; 19:746–750. [PubMed: 11479567]
15. Huang P, He Z, Ji S, et al. Induction of functional hepatocyte-like cells from mouse fibroblasts by defined factors. Nature. 2011; 475:386–389. [PubMed: 21562492]
16. Lowes KN, Brennan BA, Yeoh GC, et al. Oval cell numbers in human chronic liver diseases are directly related to disease severity. Am J Pathol. 1999; 154:537–541. [PubMed: 10027411]
17. Aharoni-Simon M, Hann-Obercyger M, Pen S, et al. Fatty liver is associated with impaired activity of PPARgamma-coactivator 1alpha (PGC1alpha) and mitochondrial biogenesis in mice. Lab Invest. 2011; 91:1018–1028. [PubMed: 21464822]
18. Dalleau S, Baradat M, Gueraud F, et al. Cell death and diseases related to oxidative stress: 4-hydroxynonenal (HNE) in the balance. Cell Death Differ. 2013; 20:1615–1630. [PubMed: 24096871]
19. Kanno S, Ishikawa M, Takayanagi M, et al. Characterization of hydrogen peroxide-induced apoptosis in mouse primary cultured hepatocytes. Biol Pharm Bull. 2000; 23:37–42. [PubMed: 10706408]
20. Garg TK, Chang JY. Oxidative stress causes ERK phosphorylation and cell death in cultured retinal pigment epithelium: prevention of cell death by AG126 and 15-deoxy-delta 12, 14-PGJ2. BMC Ophthalmol. 2003; 3:5. [PubMed: 12659653]
21. Kang KS. Abnormality on liver function test. Pediatr Gastroenterol Hepatol Nutr. 2013; 16:225–232. [PubMed: 24511518]
22. Glaser SS, Gaudio E, Rao A, et al. Morphological and functional heterogeneity of the mouse intrahepatic biliary epithelium. Lab Invest. 2009; 89:456–469. [PubMed: 19204666]
23. Poling HM, Mohanty SK, Tiao GM, et al. A comprehensive analysis of aquaporin and secretory related gene expression in neonate and adult cholangiocytes. Gene Expr Patterns. 2014; 15:96–103. [PubMed: 24929031]
24. Strnad P, Siegel M, Toivola DM, et al. Pharmacologic transglutaminase inhibition attenuates drug-primed liver hypertrophy but not Mallory body formation. FEBS lett. 2006; 580:2351–2357. [PubMed: 16616523]
25. Itoh T, Miyajima A. Liver regeneration by stem/progenitor cells. Hepatology. 2014; 59:1617–1626. [PubMed: 24115180]
26. Tarlow BD, Finegold MJ, Grompe M. Clonal tracing of Sox9+ liver progenitors in mouse oval cell injury. Hepatology. 2014; 60:278–289. [PubMed: 24700457]
27. Choi TY, Ninov N, Stainier DY, et al. Extensive conversion of hepatic biliary epithelial cells to hepatocytes after near total loss of hepatocytes in zebrafish. Gastroenterology. 2014; 146:776–788. [PubMed: 24148620]
28. He J, Lu H, Zou Q, et al. Regeneration of liver after extreme hepatocyte loss occurs mainly via biliary transdifferentiation in zebrafish. Gastroenterology. 2014; 146:789–800. e788. [PubMed: 24315993]
29. Pickens MK, Yan JS, Ng RK, et al. Dietary sucrose is essential to the development of liver injury in the methionine-choline-deficient model of steatohepatitis. J Lipid Res. 2009; 50:2072–2082. [PubMed: 19295183]
30. Alison MR, Golding M, Sarraf CE, et al. Liver damage in the rat induces hepatocyte stem cells from biliary epithelial cells. Gastroenterology. 1996; 110:1182–1190. [PubMed: 8613008]

31. Petersen B, Yee CJ, Bowen W, et al. Distinct morphological and mito-inhibitory effects induced by TGF-beta 1, HGF and EGF on mouse, rat and human hepatocytes. Cell Biol Toxicol. 1994; 10:219–230. [PubMed: 7895151]

32. Tephly TR, Gibbs AH, De Matteis F. Studies on the mechanism of experimental porphyria produced by 3,5-diethoxycarbonyl-1,4-dihydrocollidine. Role of a porphyrin-like inhibitor of protohaem ferro-lyase. Biochem J. 1979; 180:241–244. [PubMed: 486100]

33. Knight B, Yeap BB, Yeoh GC, et al. Inhibition of adult liver progenitor (oval) cell growth and viability by an agonist of the peroxisome proliferator activated receptor (PPAR) family member gamma, but not alpha or delta. Carcinogenesis. 2005; 26:1782–1792. [PubMed: 15917308]

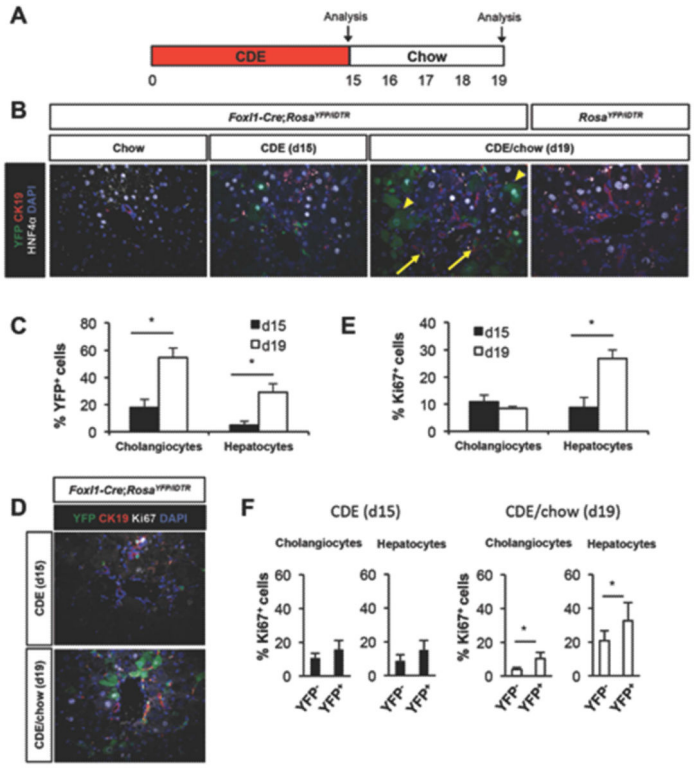

Figure 1.

Foxl-Cre-labeled cells contribute substantially to the liver parenchyma following CDE diet-mediated injury. (A) Schema of the treatment paradigm. Mice were fed a CDE diet for 15 days followed by 4 days of chow diet. (B-F) Characterization of YFP^+ cells in CDE diet treated *Foxl1-Cre*;$Rosa^{YFP/iDTR}$ mice after the injury phase (d15) and after 4 days of recovery period (d19). (B) Representative images of liver sections stained for YFP, CK19, HNF4α, and DAPI. Arrows: YFP^+CK19^+ cholangiocytes; arrowheads: $YFP^+HNF4\alpha^+$ hepatocytes. (C) Quantification of the percentage of YFP^+ cells in CDE diet-treated *Foxl1-Cre*;$Rosa^{YFP/iDTR}$ mice (n = 4 per each group). (D) Representative images of liver sections stained for YFP, CK19, Ki67, and DAPI. (E) Quantification of the percentage of $Ki67^+$ cells (n = 4-5 per each group) in CDE diet-treated *Foxl1-Cre*;$Rosa^{YFP/iDTR}$ mice. (F) Quantification of the percentage of $Ki67^+$ cells in YFP^- populations and YFP^+ populations in CDE diet-treated *Foxl1-Cre*;$Rosa^{YFP/iDTR}$ mice (n = 4 per each group). Error bars represent the standard error of the mean. $*P < .05$.

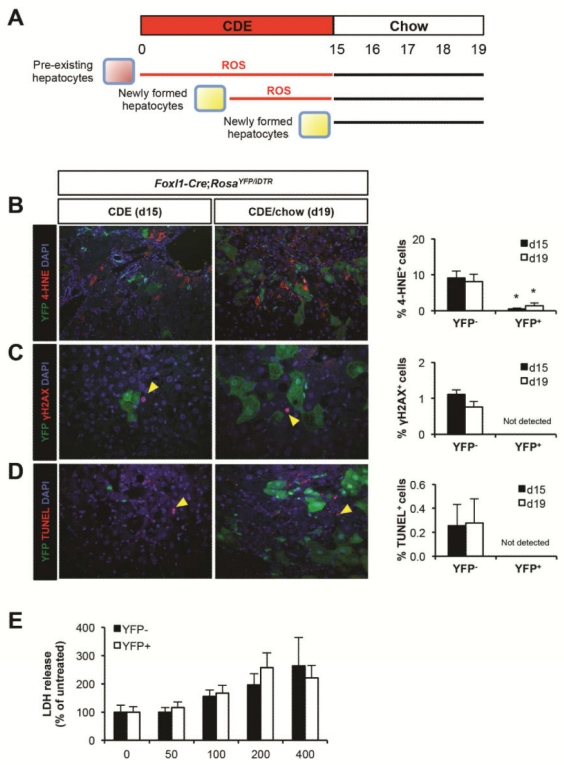

Figure 2.

YFP$^+$ hepatocytes are newly formed cells. (A) Schema illustrating how newly formed YFP$^+$ hepatocytes are exposed to reactive oxygen species (ROS) for a shorter time interval as compared to pre-existing YFP$^-$ hepatocytes. (B) Left panel: representative images of liver sections stained for YFP, 4-HNE, and DAPI. Right panel: quantification of the percentage of 4-HNE$^+$ cells in YFP$^-$ hepatocytes and YFP$^+$ hepatocytes in CDE diet-treated *Foxl1-Cre*;*Rosa*$^{YFP/iDTR}$ mice (n = 4 per each group). (C) Left panel: representative images of liver sections stained for YFP, γH2AX, and DAPI. Arrowheads: γH2AX$^+$ hepatocytes. Right panel: quantification of the percentage of γH2AX$^+$ cells in YFP$^-$ hepatocytes and YFP$^+$ hepatocytes in CDE diet-treated *Foxl1-Cre*;*Rosa*$^{YFP/iDTR}$ mice (n = 4 per each group). (D) Left panel: representative images of liver sections stained for YFP, TUNEL, and DAPI. Arrowheads: TUNEL$^+$ hepatocytes. Right panel: quantification of the percentage of TUNEL$^+$ cells in YFP$^-$ hepatocytes and YFP$^+$ hepatocytes in CDE diet-treated *Foxl1-Cre*;*Rosa*$^{YFP/iDTR}$ mice (n = 4 per each group). (E) Quantification of the percentage of lactate dehydrogenase (LDH) release from sorted YFP$^-$ hepatocytes and YFP$^+$ hepatocytes treated with hydrogen peroxide (H_2O_2) for 24 hours in culture (n = 5 per each group). Error bars represent the standard error of the mean. *P < .05, YFP$^-$ versus YFP$^+$.

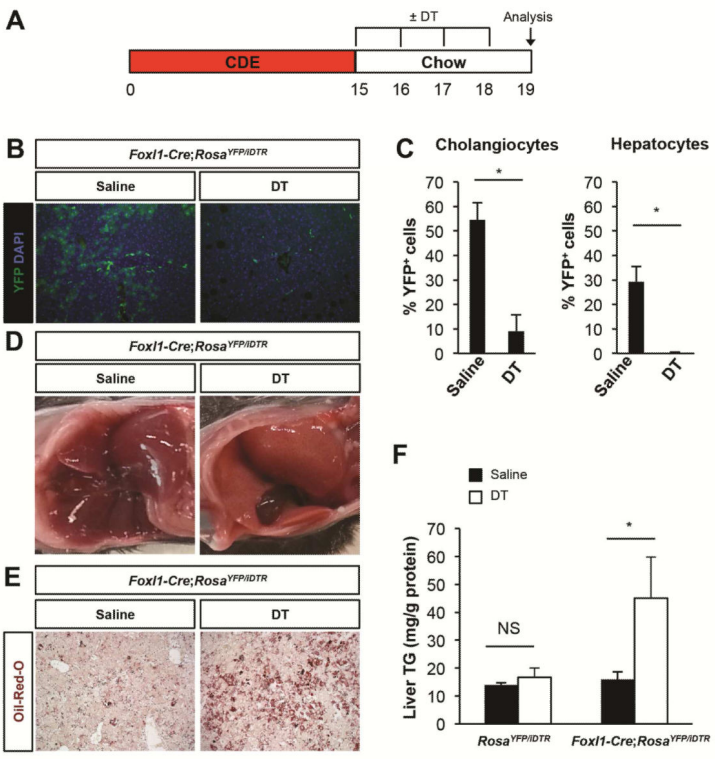

Figure 3.

Ablation of *Foxl1-Cre*/YFP$^+$ cells exacerbates hepatic steatosis following CDE diet. (A) Schema of the treatment paradigm. (B) Diphtheria toxin (DT) injection effectively ablates YFP$^+$ cells. Representative images of liver sections stained for YFP and DAPI in mice treated with saline and DT are shown. (C) Quantification of the percentage of YFP$^+$CK19$^+$ cholangiocytes and YFP$^+$HNF4α$^+$ hepatocytes (n = 4 per each group). (D) Morphology of the liver of mice treated with saline or DT. (E) Oil-Red-O staining of liver sections. (F) Analysis of hepatic triglyceride (TG) content (n = 3-6 per each group). Error bars represent the standard error of the mean. NS, not significant; *P < .05.

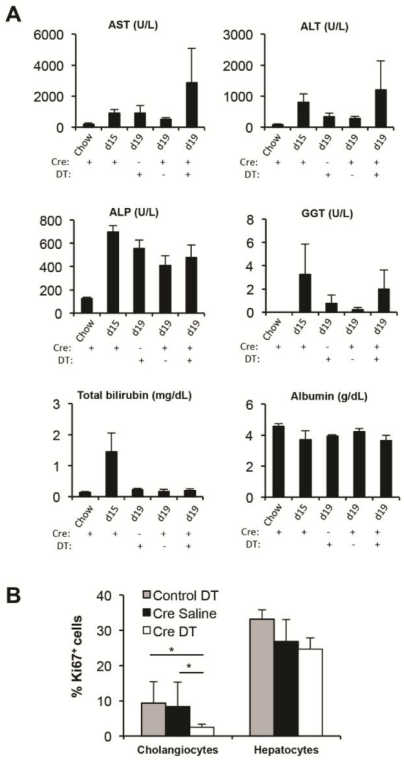

Figure 4.

Markers of liver injury and function. (A) Plasma was collected from *Foxl1-Cre*;*Rosa*$^{YFP/iDTR}$ mice (Cre+) and *Rosa*$^{YFP/iDTR}$ mice (Cre-) (n = 3-6 per each group). Mice were treated with chow, CDE diet for 15 days (d15), or CDE diet for 15 days followed by 4 days of chow (d19; recovery). Mice were treated with saline (DT-) or DT (DT+) during the 4 day recovery phase. AST, aspartate aminotransferase; ALT, alanine aminotransferase; ALP, alkaline phosphatase; GGT, gamma-glutamyltransferase. (B) Quantification of the percentage of Ki67^{+} cholangiocytes and Ki67^{+} hepatocytes in *Rosa*$^{YFP/iDTR}$ mice (control) and *Foxl1-Cre*;*Rosa*$^{YFP/iDTR}$ mice (Cre) (n = 4 per each group). Error bars represent the standard error of the mean. *$P < .05$.

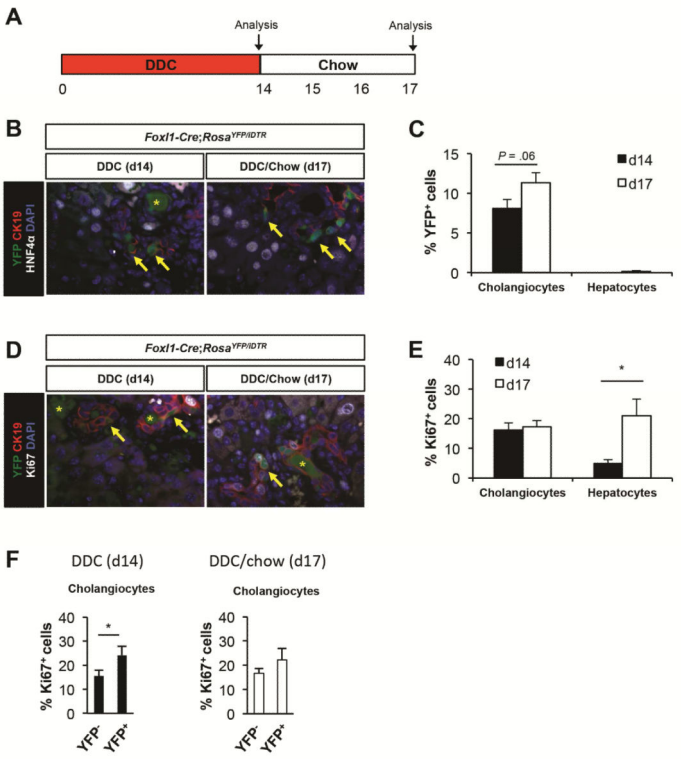

Figure 5.

Foxl-Cre-labeled cells contribute to the ductal epithelium following DDC diet-mediated injury. (A) Schema of the treatment paradigm. Mice were fed a DDC diet for 14 days followed by 3 days of chow diet. (B-F) Characterization of YFP^+ cells in DDC-diet treated *Foxl1-Cre*;$Rosa^{YFP/iDTR}$ mice after the injury phase (d14) and after 3 days of recovery (d17). (B) Representative images of liver sections stained for YFP, CK19, HNF4α, and DAPI. Arrows: YFP^+CK19^+ cholangiocytes; asterisks: porphyrin pigment plugs. (C) Quantification of the percentage of YFP^+ cells in DDC diet-treated *Foxl1-Cre*;$Rosa^{YFP/iDTR}$ mice (n = 4 per each group). (D) Representative images of liver sections stained for YFP, CK19, Ki67 and DAPI. Arrows: YFP^+CK19^+ cholangiocytes; asterisks: porphyrin pigment plugs. (E) Quantification of the percentage of $Ki67^+$ cells in DDC-diet treated *Foxl1-Cre*;$Rosa^{YFP/iDTR}$ mice (n = 4 per each group). (F) Quantification of the percentage of $Ki67^+$ cells in YFP^- populations and YFP^+ cholangiocytes in DDC-diet treated *Foxl1-Cre*;$Rosa^{YFP/iDTR}$ mice (n = 4 per each group). Error bars represent the standard error of the mean. **P* < .05.

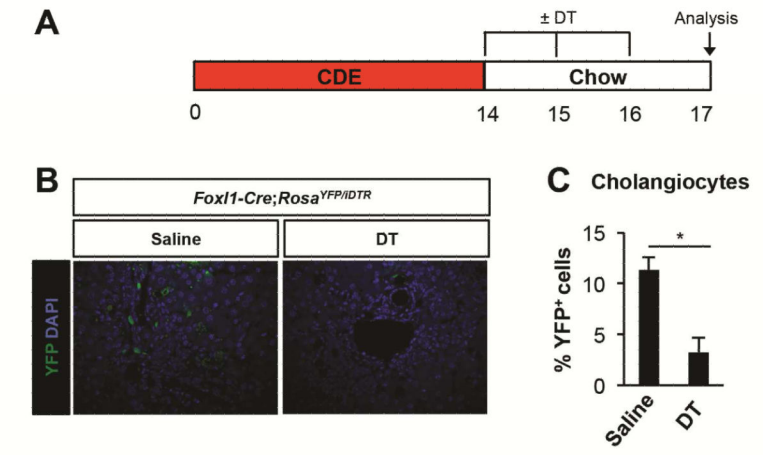

Figure 6.

Ablation of *Foxl1-Cre*/YFP^{+} cells in the liver of mice fed a DDC-diet. (A) Schema of the treatment paradigm. (B) Diphtheria toxin (DT) injection effectively ablates YFP^{+} cells. Representative images of liver sections stained for YFP and DAPI in mice treated with saline and DT are shown. (C) Quantification of the percentage of YFP^{+}CK19^{+} cholangiocytes after DT treatment or in saline-treated controls (n = 4 per each group). Error bars represent the standard error of the mean. *$P < .05$.

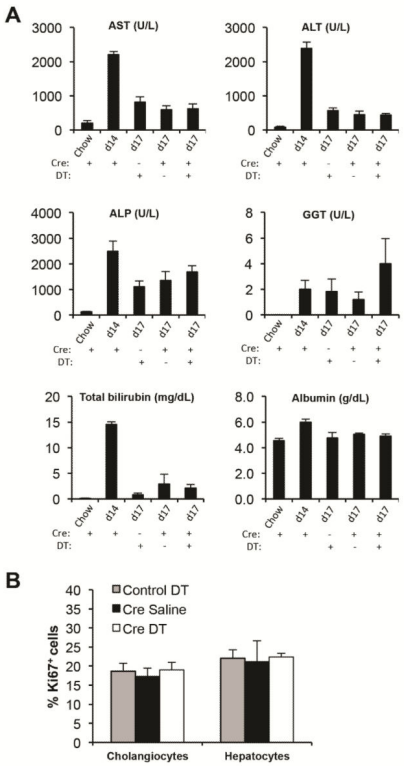

Figure 7.

Markers of liver injury and function in mice treated with DDC. (A) Plasma was collected from *Foxl1-Cre*;*Rosa*$^{YFP/iDTR}$ mice (Cre+) and *Rosa*$^{YFP/iDTR}$ mice (Cre-) (n = 6 per each group). Mice were treated with chow, DDC diet for 14 days (d14), and DDC diet for 14 days followed by 3 days of chow (d17). Mice were treated with saline (DT-) or DT (DT+) during the recovery phase. (B) Quantification of the percentage of Ki67^{+} cholangiocytes and Ki67^{+} hepatocytes in *Rosa*$^{YFP/iDTR}$ mice (control) and *Foxl1-Cre*;*Rosa*$^{YFP/iDTR}$ mice (Cre) at d17 (n=4 per group). Error bars represent the standard error of the mean.